

Research Paper

Nerve modulation therapy in gouty arthritis: targeting increased sFRP2 expression in dorsal root ganglion regulates macrophage polarization and alleviates endothelial damage

Jingtian Mei*, Feng Zhou*, Han Qiao, Hanjun Li, Tingting Tang✉

Shanghai Key Laboratory of Orthopaedic Implants, Department of Orthopaedic Surgery, Shanghai Ninth People's Hospital, Shanghai Jiao Tong University School of Medicine, Shanghai, PR China.

*These authors contributed equally to this work

✉ Corresponding author: Tingting Tang, tt@sjtu.edu.cn, Tel/fax: +8621 6313 7020

© Ivyspring International Publisher. This is an open access article distributed under the terms of the Creative Commons Attribution (CC BY-NC) license (<https://creativecommons.org/licenses/by-nc/4.0/>). See <http://ivyspring.com/terms> for full terms and conditions.

Received: 2019.02.08; Accepted: 2019.04.17; Published: 2019.05.31

Abstract

Gouty arthritis (GA) is a form of arthritis caused by uric acid deposition in the joints that result in intense inflammation and pain. Accumulating evidence showed the importance of the sensory neurons signal upon immune cells by releasing neuropeptides and chemokines to regulate associated immune-inflammatory response. In this study, we investigated the significance of sensory neuron neuropeptides and chemokine signals on inflammation-induced macrophages polarization during GA.

Methods: We screened the mRNA expression profile during GA in dorsal root ganglion (DRG) neurons to identify the most likely candidate that mediates the neuro-immune communication. Then, we silenced specific gene expression in the DRG by lentiviral vectors in the monosodium urate (MSU)-induced ankle GA mouse model and evaluated alterations in the inflammatory response. In vitro, primary macrophages were used to investigate the neural impact on M1/M2 subtype polarization, proinflammatory cytokine production and downstream endothelial damage. Mechanism by which macrophage inflammation is induced in the DRG was evaluated by Western blot, immunofluorescence, and immunoprecipitation.

Results: We found that secreted frizzled-related protein 2 (sFRP2) was the most upregulated gene in dorsal root ganglion (DRG) neurons in response to monosodium urate (MSU) deposition. Injection of LV-sFRP2-shRNA into the L4 and L5 DRG significantly suppressed inflammatory cell infiltration and M1 polarization in the synovial membrane, attenuating hyperalgesia and ankle swelling in the GA mouse model. In vitro, DRG neurons-derived sFRP2 promoted M1 polarization and macrophage migration, thereby upregulating the production of proinflammatory cytokines and preventing endothelial apoptosis. Furthermore, DRG-derived sFRP2 activated the nuclear factor (NF)- κ B pathway by destabilizing the β -catenin and p65 complex.

Conclusion: We demonstrated the involvement of a sensory neuron-macrophage axis in GA pathology that was regulated by sFRP2 expression in a paracrine manner. Targeting increased sFRP2 expressions in DRG provide novel insights for future GA research in both pain alleviation and treatment of gout inflammation.

Key words: Dorsal root ganglion, Gout, sFRP2, Macrophages, Wnt/ β -catenin

Introduction

Gouty arthritis (GA), with an increasing prevalence of >1% in most developed countries, has distinguished itself as the most common and

disabling musculoskeletal complaint [1]. As a consequence of a chronic disturbance and elevation in the hyperuricemia level, GA occurs directly due to the

deposition of monosodium urate (MSU) crystals in articular and periarticular tissues, leading to acute joint inflammation [2]. Resident macrophages or monocytes have been shown to react to the deposited MSU crystals through toll-like receptor 2 (TLR2) and TLR4 [3, 4], indicating a pivotal role in the initiation of the inflammatory cascade of macrophages by MSU crystals. Macrophages acquire a proinflammatory M1 phenotype instead of an anti-inflammatory M2 phenotype after MSU stimulation [5, 6]. Subsequently, endothelial cells are activated and impaired by these inflammatory mediators [7, 8]. After M1 macrophage-endothelial cell damage in GA, M2 macrophages are involved in tissue remodeling and repair [9, 10].

As an interesting feature of gout, the process of inflammation is recognized as a self-limited attack, which spontaneously resolves within ten days without medical interventions [11], providing a potential to develop novel therapies targeting the mechanisms of spontaneous resolution in acute GA. Herein, a range of potential shutdown mechanisms, such as crystal binding of apolipoprotein B/E (Apo B/E) [12], chemokine depletion [13], and neutrophil apoptosis [14], have been proposed. Nonetheless, certain disturbing stimuli within the GA microenvironment, such as inflammatory synovial, irritated nerve and dysfunctioning endocrine reactions, inevitably result in the disruption of arthritis homeostasis. Additionally, little is known about these primary regulators that propel such significant macrophage M1/M2 polarization after MSU deposition in GA, encouraging the launch of numerous in-depth preclinical studies in GA.

GA is initially characterized by violent and sudden pain together with swelling and redness, indicating the activation of the nervous system during inflammation. In addition to the apparent activation of pain induction, studies have also revealed interactions between the nervous and inflammatory system [15, 16]. Histologically, inflammatory cells in GA, such as macrophages, mast cells, and neutrophils, are mostly located in proximity to peripheral nerve fibers. Once macrophages recognize extracellular noxious stimuli, they release soluble factors that lead to the sensitization of peripheral nociceptive nerves directly [17]. A previous study demonstrated significant macrophage infiltration into the ipsilateral and contralateral lumbar dorsal root ganglion (DRG) in a mouse model of antigen-induced arthritis, resulting in the generation of hyperalgesia on bilateral sides [18]. Furthermore, inflammatory cells are also regulated by the nervous system. The action potential that mediates the sensation of pain stimulates the release of neuropeptides such as calcitonin

gene-related peptide (CGRP) and substance P, which bind to receptors expressed on innate immune cells such as macrophages to activate inflammation [19]. Borovikova et al. demonstrated that the activation of vagus nerves could inhibit endotoxin-induced M1 macrophage polarization, polarizing macrophages to the M2 phenotype via the activation of Janus kinase 2 (JAK2)/ signal transducer and activator of transcription protein 3 (STAT3) transcription factors [20]. G. Trevisan et al. reported that the ongoing GA-elicited nociception and inflammatory response was reduced by blockade of transient receptor potential ankyrin 1 (TRPA1) expressed on primary sensory neurons [21]. These observations suggest an intimate linkage between sensory nerves and GA. However, the underlying mechanism by which sensory nerves influence the inflammatory process of macrophages, especially M1/M2 polarization, is not fully understood.

Currently, targeting DRG hold a great promise for the precise and long-lasting treatment of pain without debilitating central nervous system (CNS) [22]. Opposed to the blood-brain barrier in the CNS, DRG and peripheral axons lack an efficient neurovascular barrier [23]. Additionally, the permeable connective tissue capsule and high density of blood capillaries in ganglion allow various therapeutic or diagnostic approaches targeting DRG including systemic administration, local injections, stem cell therapy, and siRNA therapy [24-26].

Regulating approximately 400 genes, Wnt/ β -catenin signaling pathway was involved in cell growth, immune function, differentiation, and apoptosis [27]. sFRP proteins (sFRP1-sFRP5) appear to represent the largest family of Wnt modulators [28]. Here, we first found that secreted frizzled-related protein 2 (sFRP2) from DRG neurons was the primary regulator modulating the subsequent MSU-induced macrophage M1/M2 polarization. Accordingly, we presented an RNA interference strategy to relieve the inflammatory response of GA by silencing sFRP2 expression in DRG neurons both in vivo and in vitro. Our work highlighted the essential role of sensory nerves in macrophage polarization through their secretion of sFRP2 to activate macrophages via a Wnt- β -catenin/NF- κ B interaction, further attenuating the inflammatory damage of endothelial cells in GA, undoubtedly providing a valid target for future GA treatment.

Materials and Methods

C57BL/6 mice (6-week-old, male) were purchased from Shanghai SIPPR-Bk Lab Animal Co., Ltd. and maintained in specific-pathogen-free laboratory animal facilities of Shanghai Ninth

People's Hospital. All mice were acclimated to the facility for seven days before the *in vivo* experiment. For the isolation of primary mouse sensory neurons and macrophages, C57BL/6 mice (male, 4-week-old) were sacrificed by an anesthesia overdose.

All the experimental procedures and the animal care protocols above were reviewed and approved by the Institution of Animal Care and Use Committee (IACUC) of Shanghai Ninth People's Hospital. All mice were allowed *ad libitum* access to food and water prior to and throughout the experimental protocol.

Cells, Media, and Reagents

For the isolation of primary mouse sensory neurons, DRGs from all spine levels were dissected and subjected to an enzyme mixture of 0.1% collagenase (Sigma-Aldrich, SCR103), 200 U/mL DNase (Sigma-Aldrich, 10104159001), 0.25% trypsin (Sigma-Aldrich, T2600000) at 37 °C for 45 min. Next, the myelin sheath and undesired cells were partially depleted through a 5-min 200 g density-gradient centrifugation with 15% percoll (Biosharp, 10243024). Primary sensory neurons were suspended in DMEM/Ham's F12 1:1 mixture medium containing 10% FBS, N2 supplements (Gibco, 1950299) and 50 ng/mL β -NGF (Peprotech, 450-01). 100 μ M Ara-C (Sigma-Aldrich, C1768) was supplemented to inhibit the proliferation of non-neuronal cells and then removed two days before the further experiment.

Bone marrow-derived macrophages (BMMs) were expelled from the femur and tibiae of mice. After 1-day culture in MEM- α with 10% FBS, 30 ng/mL M-CSF (R&D Systems, Q3U4F9), suspension cells were seeded into 6-well plate. For macrophage differentiation, cells were cultured in the aforementioned culture media for five days until further treatment. M0 were polarized into M1 using 20 ng/mL LPS (Sigma-Aldrich, L2630) plus 20 ng/mL IFN- γ (Peprotech, 315-05), and into M2 using 20 ng/mL IL-4 (Peprotech, 214-14) for two days.

The serum-free MEM- α media was replaced for 24 h to generate conditioned medium. The conditioned medium was filtered with 0.2 μ m micron syringe filter to avoid cross-contamination of cells. For subsequent cell culture, conditioned medium was diluted 1:1 with fresh culture medium. For Luminex assay, the conditioned medium of stimulated macrophages was collected as above mentioned. The assay was conducted according to manufacturer's protocol using Bio-Plex Pro Mouse Cytokine Grp (#M60009RDPD) with Luminex 200 system (Austin, TX, USA) in Wayen Biotechnologies Shanghai, Inc.

HUVEC (HUVEC-20001) were purchased from Cyagen Biosciences and cultured in MEM- α

(Invitrogen, 11090081) supplemented with 10% FBS.

MSU crystals were purchased from Sigma-Aldrich and prepared as described before [29].

Lentivirus Transduction *in vitro* and *in vivo*

The culture of mice DRG neurons was prepared as above-mentioned. Next, cell cultures were transduced with various modified lentivectors in the presence of 6 μ g/mL polybrene (Solarbio, H8761). Twenty-four hours after the onset of transduction, we removed the viruses and replaced with a supplemented neurobasal medium. After 72 h culture, direct ZsGreen1 fluorescence was examined and photographed under a fluorescence microscope to determine the transduction efficiency of various lentivirus-vectors on mice DRG neurons.

The DRG transduction *in vivo* was performed as previously described [30]. In brief, we anesthetized the mice with 1% pentobarbital sodium at a dose of 50 mg/kg. The paraspinal muscles of the lower lumbar were separated to expose the L4-L5 intervertebral foramina for microinjection. Lentiviral preparations (5×10^8 units per mL) were 1:1 diluted with 20% mannitol. Then mice were injected either 2 μ L lentiviral preparations or saline, in both cases containing 100 ng polybrene, into both L4 and L5 DRGs unilaterally. Thus, the virus load was 1×10^6 transfection units for each mouse.

The animal model of MSU-induced ankle gouty arthritis

One week after the *in vivo* transduction procedure, all the mice of the transfected and control groups were anesthetized. And then administered 20 μ L MSU crystals (10 mg/mL) into the ankle joint of the right lower limb to establish an animal model of ankle gouty arthritis. The circumferences and paw withdrawal threshold of injected ankle joints were measured after 1, 3, and 5 days after the MSU injection. Subsequently, five mice of each group were sacrificed for histological evaluation.

Sequencing

After establishing MSU-induced ankle gouty arthritis successfully, total RNA was extracted from DRGs of control and GA mice using TRIzol reagent (Invitrogen, 15596026) according to the manufacturer's instructions. The Agilent 4200 TapeStation system offered the sample quality control for the full range of sizing applications for RNA. Paired-end reads were obtained on an Illumina PE150 in Shenzhen HaploX Biotechnology Co., Ltd. The program of Hierarchical Indexing for Spliced Alignment of Transcripts (HISAT2) was used to align the reads to the UCSC mm10 mouse reference genome. The transcript abundance (represented by

Reads Per Kilobase Million, RPKM) was measured. Genes and transcripts with RPKM values lower than five were excluded from the analysis. R (3.0.2) generated the Pearson correlation analysis and heatmaps.

Histological Evaluation

Synovial tissues and DRGs were dissected and immersed into 4% paraformaldehyde in PBS for 4 h. Then explants were embedded in O.C.T. compound (Tissue-Tek, 4583) frozen next to a cryoprotection in a solution of 20% sucrose overnight in room temperature. For immunofluorescent staining, the ankle joint specimens were sagittally sectioned to obtain free-floating 50- μ m-thick slices for a better vision of nerve fibers in synovial tissue of ankle joint, while DRG explants were sectioned to regular 3.5- μ m-thick slices and both stained for β -III-Tubulin (Cell Signaling Technology, D71G9, 1:400), sFRP2 (Abcam, ab86379, 1:100) in Eppendorf tube. For staining of M1/M2 macrophages in synovial tissue, 3.5- μ m-thick slices were obtained for CD16/32 (Abcam, ab25235, 1:20), CD206 (Abcam, ab64693, 1:100) and hematoxylin and eosin staining.

Zeiss LSM710 confocal microscope was used for confocal imaging of samples at an original magnification $\times 40$ and Zen software.

Von Frey

We used von Frey to test the pain behavior of mice as previously described in detail [31]. The technician was blinded to the treatment to ensure the randomization of the test. The test started with the presentation of the 0.4 g filament and place onto a mid-plantar surface of the hind paw of the mouse until it bends. Presented and subsequent presentations of filaments are presented consistent with the "up-down" method. Then the 50% paw withdrawal threshold was calculated using the formula:

$$50\% \text{ threshold (g)} = 10(X+kd) / 10^4$$

X = the value (in log units) of the final von Frey filament, k = tabular value for the response pattern and d = the average increment (in log units) between von Frey filaments.

Phenotypic Characterization of M1/M2 Macrophages

To assess the polarization of macrophages into M1 or M2 phenotype, cytokines or MSU crystal-treated primary BMMs were harvested, washed with PBS and incubated with blocking buffer (1% goat serum and 1% BSA in PBS). Cells were stained with CD68 (BD Horizon, 566388), CD16/32 (BD Pharmingen, 561727, 2 μ g/mL), CD206 (BD

Pharmingen, 565250, 2 μ g/mL) according to the manufacturer's protocol. A FACScan flow cytometer (BD, CA, USA) was further used to analyze samples.

Immunocytochemistry was performed to access the specific markers in macrophages. Macrophages were fixed in 4% paraformaldehyde, blocked and penetrated with blocking buffer (1% goat serum, 1% BSA and 0.1% Triton X100 in PBS). Then cells were incubated with CD16/32 (Abcam, ab25235, 10 μ g/mL), CD206 (Abcam, ab64693, 1:2000) overnight at 4°C, followed with corresponding secondary antibody (goat anti-rat IgG (Abcam, ab150157, 1:1000), goat anti-rabbit IgG (Abcam, ab150080, 1:1000)) for 2 h at room temperature. Images were acquired with Zeiss LSM710, analyzed with Zen software.

Migration Assay

Eight μ m-pore transwell inserts (Corning, CLS3428) were coated with Matrigel matrix (BD Life Sciences, 356234) which was 1:4 diluted with MEM- α . 700 μ L of conditioned media was added to each well of a 24-well plate followed by addition of coated inserts. We added 10^5 BMMs to each inserts and cultured in 5% CO₂ at 37 °C for 12 h for migration. MCP-1 (Peprotech, 250-10, 20 ng/mL), 200 μ g/mL MSU, and conditioned medium of DRGs were used. Then inserts were washed and fixed with 4% paraformaldehyde followed by staining with 0.2% crystal violet (Sigma-Aldrich, C6158). Cells on the top of the insert were removed using a cotton swab and only cells which migrated across the membrane were quantitated. The membranes of the transwell insert were carefully cut using a scalpel. The digital images were taken with Olympus IX71. Cell numbers were counted with Image J software.

HUVECs Apoptosis Analysis

5×10^5 HUVECs were seeded in a 6-well plate and stimulated with following media. Group1, complete media; Group 2, 1:1 mixture of complete and conditioned medium from macrophages stimulated with 200 μ g/mL MSU; Group 3, 1:1 mixture of complete and conditioned medium from cocultured DRG and macrophages stimulated with 200 μ g/mL MSU; Group 4, 1:1 mixture of complete and conditioned medium from cocultured shRNA-transduced DRG and macrophages stimulated with 200 μ g/mL MSU.

Cell apoptosis rates of HUVECs were determined by flow cytometry via Annexin V/PI staining as previously described [32].

TUNEL staining was performed using TUNEL apoptosis assay kit (Beyotime, C1086) according to manufacturer's protocols. TUNEL-positive cells were identified by the presence of fluorescence.

Quantitative RT-PCR

RNA of different groups of DRG neurons, macrophages, HUVEC were extracted using TRIzol reagent (Invitrogen, 15596026) according to the manufacturer's instructions. Briefly, after Trizol, we added chloroform and centrifuged at 4°C 12000 g for 15 min and separated the upper clear aqueous phase containing RNA. Add 0.5 mL of isopropanol to the aqueous phase, incubated for 10 min. Then we centrifuged for 10 min at 12000g following washing twice with 75% ethanol. Next, cDNA synthesis was performed using random hexamers, and qPCR was carried out using SYBR® Premix Ex Taq™ (Takara Bio, RR420A) on a real-time PCR system (Applied Biosystems, USA, ABI 7500). We normalized gene expression to the geometric mean of GAPDH. The primers used are listed in the Table S1.

Western Blot and ELISA Analysis

Macrophages treated with MSU and conditioned medium from DRG were lysed in RIPA buffer (Beyotime, P0013C) supplemented with 1 mM PMSF (Beyotime, ST506). We also aliquoted DRG neurons culture supernatant for sFRP2 enzyme-linked immunosorbent assay (ELISA) analyses (LifeSpan Biosciences, LS-F34960). The following antibodies were used to detect proteins. β -catenin (Cell Signaling Technology, 8480, 1:1000), sFRP2 (Abcam, ab86379,1:500), Wnt9a (Abcam, ab125957, 1:1000), FZD2 (Abcam, ab109094, 1:1000), DVL2 (Abcam, ab124933, 1:1000), Cyclin D1 (Cell Signaling Technology, 2978, 1:1000), C-myc (Cell Signaling Technology, 5605, 1:1000), p-I κ B α (Cell Signaling Technology, 2859, 1:1000), I κ B α (Cell Signaling Technology, 2859, 1:1000), p65 (Cell Signaling Technology, 8242, 1:1000), Histone H3 (Cell Signaling Technology, 4499, 1:1000), GAPDH (Cell Signaling Technology, 5174, 1:1000). Secondary antibodies included goat anti-rabbit IgG (Invitrogen, 35568, 1:30000), goat anti-mouse IgG (Invitrogen, G-21040, 1:30000).

We performed western blotting as previously described [33], and the relative intensities of bands were normalized to those of GAPDH or Histone H3 bands.

Co-IP

Macrophages were cultured in control, 200 μ g/mL MSU and 200 μ g/mL MSU in conditioned medium from DRG. Total cell lysates were incubated overnight at 4 °C with P65 (Cell Signaling Technology, 8242, 5 μ g) or normal IgG (Cell Signaling Technology, 2729, 5 μ g) as a control. Antibody-antigen complexes were precleared with Crosslink Magnetic IP/Co-IP Kit (Thermo Fisher

scientific, 88805). After several washes, samples were boiled and analyzed by immunoblot.

Statistical Analysis

For in vitro study, experiments were conducted in biological triplicate. For in vivo experiment, five mice were assigned for each group, and 40 mice were used in total. The results were presented as the means \pm standard deviation after analyzed by the SPSS 13.0 software (Statistical Package for the Social Science, USA). Parametric data were analyzed using a Student's t-test or one-way ANOVA followed by a post hoc Tukey's test to compare two groups. The level of significance was set at $P < 0.05$ and indicated by "#" for the comparison between the vehicle group and control group and "*" for the comparison between the treated group and vehicle group. $P < 0.01$ was indicated by "**" for the comparison between the treated group and vehicle group.

Results

MSU crystals induce sFRP2 production in DRG neurons

Primary DRG neurons were dissected from control and MSU crystal-induced acute GA mice, and an RNA-Seq assay and expression profiling were performed (Figure 1A) The *Sfrp2* gene, which encodes the sFRP2 protein, a soluble modulator of Wnt signaling, was among the most upregulated genes. Next, primary DRG tissues were isolated and purified for in vitro experiments. Immunostaining of the neuro-specific marker PGP9.5 was performed to identify the cell morphology (Figure 1B) [34]. After seven days of treatment with an anti-mitotic reagent, the cell cultures comprised mostly neurons, with less than 1% nonneuronal cells, showing a high purity of DRG neurons for the subsequent experiment (Figure 1C). Next, a cell viability assay was performed to determine the cytotoxicity of MSU crystals against DRG neurons. In Figure 1D, MSU crystals did not exhibit cytotoxicity against DRGs at concentrations from 12.5 to 200 μ g/mL after 24 h treatment. Therefore, 200 μ g/mL MSU crystals were utilized for subsequent studies. RT-PCR revealed a significant 7.9 ± 0.4 elevation in *Sfrp2* mRNA expression in DRG neurons treated with 200 μ g/mL MSU crystals for 24 h (Figure 1E), in contrast with the relatively milder elevation in *Ngf*, *Enpg2*, *Ereg*, *Ptgs*, *Mmp9*, and *Grem1* expression. Furthermore, the protein expression of sFRP2 in DRG neurons was also evaluated, which was in consist with the immunofluorescence staining in Figure 1F. Additionally, Figure 1G illustrated that, in comparison with the control group, the group

exposed to 24 h stimulation with MSU crystals exhibited a 6.1 ± 0.7 -fold increase in sFRP2 expression in DRG neurons in vitro. Because sFRP2 is a secretory protein of DRG neurons, an ELISA was also performed. As shown in Figure 1H, MSU crystals induced a potent production of sFRP2 from DRG in a dose-dependent manner.

Virus-mediated shRNA knockdown of sFRP2 in the DRG attenuates inflammation in GA

To further evaluate the potential role of sFRP2 in vivo, we injected 2 μ l of the lentiviral preparation/normal saline into the L4 and L5 DRG to deliver the vector targeting sFRP2 in mice (Figure S1). Three weeks after the in vivo transduction, the animal model of MSU-induced GA was established by injecting MSU crystals into the ankle of the ipsilateral hind paw. To evaluate the transduction efficiency in vivo, the injected DRG sections (L4 and L5) were isolated. Representative images (Figure 2A) of

sections from the infected DRG show positive ZsGreen1 expression colocalized with β III-tubulin, demonstrating that LV-sFRP2-shRNA1 was capable of transducing DRG neurons in vivo. Additionally, MSU crystal injection significantly induced sFRP2 expression in the DRG. In contrast, sFRP2 expression was obviously suppressed in the sFRP2 knockdown (KD) group compared to that in the sham group, and this suppression was not affected by MSU stimulation. Next, we stained ankle joint sections to examine the nerve innervation of the synovial membrane. The confocal images revealed a similar pattern of sFRP2 expression in peripheral nerve fibers within the synovium (Figure 2B), indicating that the escalated expression of sFRP2 was found both in vertebrate DRG cells and synovial tissues, though sFRP2 was not significantly changed in the immune cells in synovium (Figure S2).

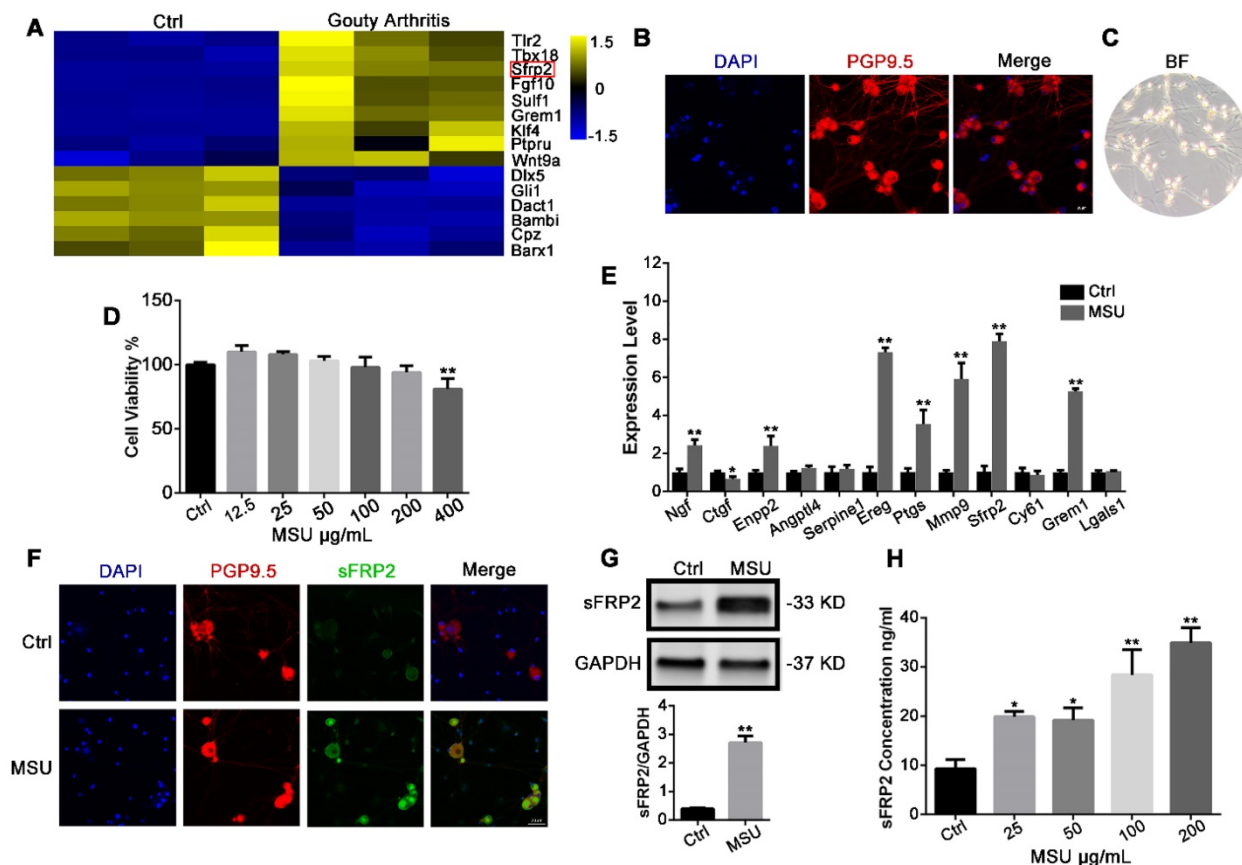


Figure 1. MSU crystals induce sFRP2 production in DRG neurons. (A), Heat map representation of RNA-Seq results. The left and right three rows represent three replicates of the expression level in the DRG from control and GA mice. Yellow represents upregulation. Blue represents downregulation. (B), Confocal images of purified DRG neurons. PGP9.5 was used as a neuron marker (red). Cell nuclei were stained with 4' 6-diamidino-2-phenylindole (DAPI; blue). Scale bar, 20 μ m. (C), Classical microscopy image of DRG neurons. (D), CCK-8 assay was performed on DRG neurons treated with varying MSU concentrations. (E), qPCR analysis of a series of the most upregulated or abundantly expressed genes of DRG neurons in response to 200 μ g/mL MSU treatment for 24 h. (F), Upregulation of sFRP2 expression in DRG neurons in response to 200 μ g/mL MSU treatment for 24 h. PGP9.5 was used as a neuron marker (red). Cell nuclei were stained with DAPI (blue). Scale bar, 20 μ m. (G), Validation of sFRP2 expression by Western blotting in DRG neurons. (H), Measurement of sFRP2 secretion in CM from DRG neurons treated with 200 μ g/mL MSU for 24 h. In vitro experiments were conducted in biological triplicate. Values are the means \pm SD (**P < 0.05 compared with control. **P < 0.01 compared with control). All statistical significance was determined using one-way ANOVA and Tukey's post comparison test.

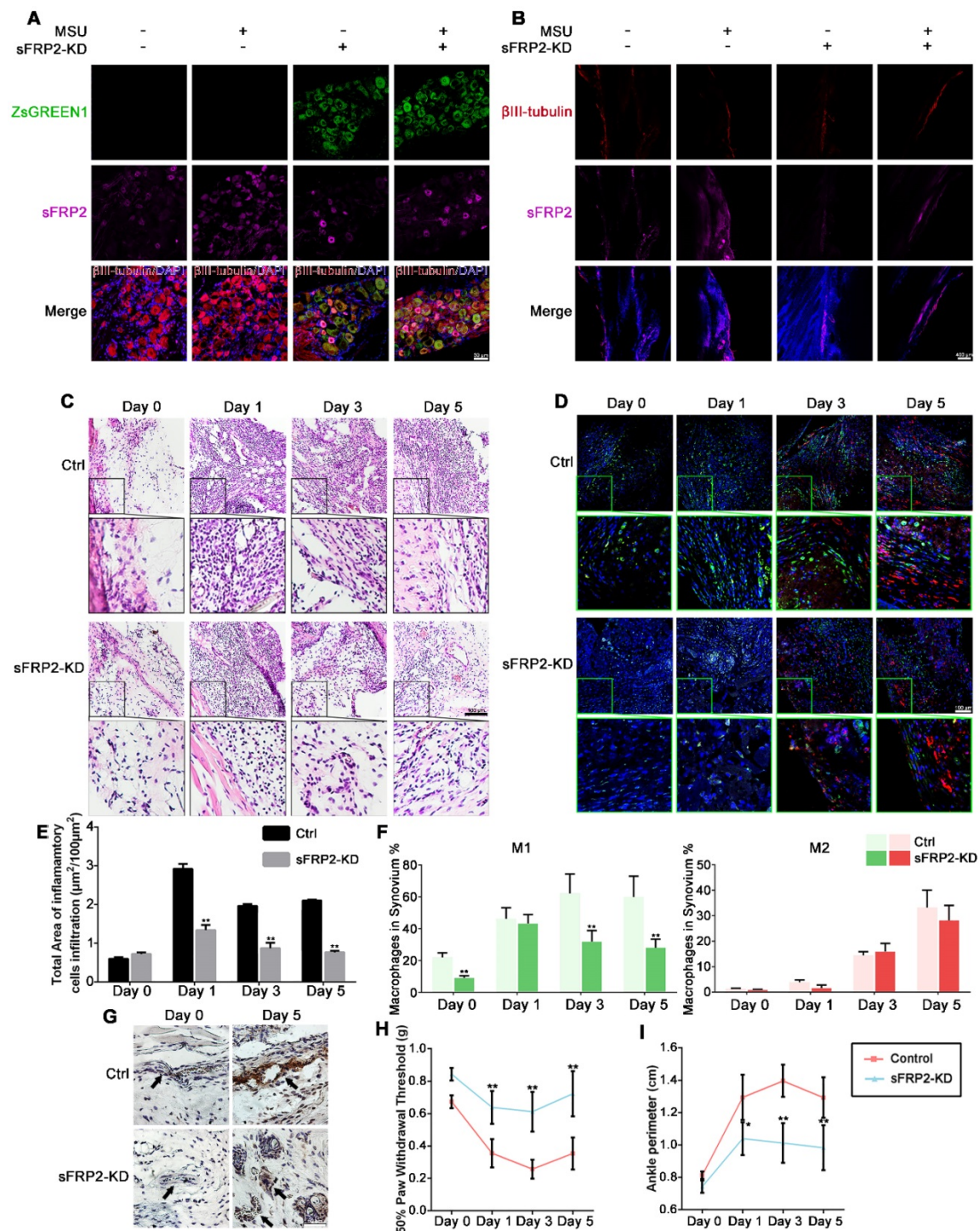


Figure 2. Virus-mediated shRNA KD of sFRP2 in DRG attenuates inflammatory attack in GA. (A), Representative images of immunofluorescence staining of ipsilateral L4 DRG sections dissected from control and transduced mice 1 day after injection of MSU crystals or normal saline. The upper panels show immunostaining for ZsGreen1 (green) in each group. The panels on the 2nd line show the sFRP2 expression level (magenta). β III-tubulin was used as a neuron marker (red). The lower panels show the merged images of ZsGreen1, sFRP2, β III-tubulin, and DAPI in each group. Scale bar, 30 μ m. (B), Representative images of immunofluorescence staining of synovial membrane sections of the ipsilateral ankle joint dissected from control and transduced mice 1 day after injection of MSU crystals or normal saline. The upper panels show immunostaining for β III-tubulin (red) in each group. The panels on the 2nd line show the sFRP2 expression level (magenta). The lower panels show the merged images of β III-tubulin, sFRP2, and DAPI in each group. Scale bar, 400 μ m. (C), Histological analyses of synovial membrane sections of control and transduced mouse ankle joints 0, 1, 3, and 5 days after injection with MSU crystals. Scale bar, 100 μ m. (D), Representative images of immunofluorescence staining of synovial membrane sections from control and transduced mouse ankle joints 0, 1, 3, and 5 days after injection with MSU crystals. CD116/32 was used as an M1 macrophage marker (green). CD206 was used as an M2 macrophage marker (red). Scale bar, 100 μ m. (E), Quantitation of immune cells infiltration in synovium membrane sections. (F), Quantitation of M1 and M2 macrophages in the synovium in the GA animal model. (G), Histological analyses of endothelial cell apoptosis in the synovial membrane of control and transduced mice five days after injection of MSU crystals or normal saline. The endothelium was characterized as a single layer of flat scale-shaped cells. Scale bar, 50 μ m. (H), Hind paw withdrawal responses in control and transduced mice 0, 1, 3, and 5 days after injection with MSU crystals. (I), Perimeter assessments of control and transduced mouse ankle joints 0, 1, 3, and 5 days after injection with MSU crystals and corresponding drugs. Values are the means \pm SD (* P < 0.05 compared with control; ** P < 0.01 compared with control (t-test)). All statistical significance was determined using one-way ANOVA and Tukey's post comparison test.

Figure 2C and 2E illustrates the infiltration of inflammatory cells in synovial membranes, which was profoundly increased due to MSU crystal treatment. Interestingly, the synovial membranes of the sFRP2 KD group showed less inflammatory cell infiltration, especially on the fifth day, than did those of the control group, indicating that sFRP2 in DRG neurons might participate in the inflammation resolution in GA. Subsequently, we identified M1 (green) and M2 (red) macrophages in the synovial membrane by immunofluorescence staining of CD16/32 and CD206 accordingly (Figure 2D). We found that the synovium of the sFRP2 KD group presented no substantial difference in M2-type macrophages compared to that of the control group. In contrast, a significant reduction in M1-type macrophages was observed (Figure 2F), suggesting that the absence of sFRP2 in the DRG exerted an inhibitory effect on M1-macrophage polarization in the synovial tissue of the GA model.

We also observed apoptosis of endothelial cells within the synovial membrane by TUNEL immunostaining. In Figure 2G, compared with the control group, the sFRP2 KD group exhibited fewer apoptotic endothelial cells. As shown in Figure 2H, compared with the group exposed to MSU alone, the sFRP2 KD group exhibited a significant increase in the 50% paw withdrawal threshold on days 1, 3, and 5, suggesting lower mechanical hyperalgesia in sFRP2 KD mice. The determination of the ankle perimeter revealed that the sFRP2 KD group had significantly less ankle swelling than the MSU alone group on the 3rd and 5th day (Figure 2I and Figure S3), demonstrating a pivotal role of sFRP2 in GA inflammation regulation.

Neural regulation of macrophage polarization and migration

Bone marrow-derived macrophages (BMMs) were induced by macrophage colony-stimulating factor (M-CSF) to differentiate into macrophages, resulting in a higher expression of F4/80 and lower expression of CD14. Hence, BMMs were seeded and cultured in conditioned medium (CM) from DRG neurons in the presence of MSU crystals at a nontoxic concentration to determine the effect of DRG-derived sFRP2 on macrophage polarization (Figure S4).

The expression of M1-associated genes, including interleukin (IL)-6, tumor necrosis factor (TNF)- α , inducible nitric oxide synthase (iNOS), and IL-12b, as well as M2-associated genes, including transforming growth factor (TGF)- β , arginase (Arg)-1, transglutaminase 2 (TGM2), and IL-10, was determined to assess the expression profile of macrophages (Figure 3A). We found significantly

higher mRNA expression of M1-associated genes in MSU-treated BMMs than in untreated BMMs. Additionally, the expression of M1-associated genes increased further with the application of DRG CM, while treatment with sFRP2 KD DRG CM inhibited the increase in the expression of IL-6, iNOS, and IL-12. For M2-associated genes, MSU promoted TGF- β and Arg-1 expression but did not affect the expression of TGM2 or IL-10. Compared with treatment with DRG CM, treatment with sFRP2 KD DRG CM prevented the downregulation of M2-associated genes. To better characterize the inflammatory profile, the conditioned medium of stimulated macrophages was analyzed by Luminex system. A similar change pattern of cytokines was shown in Figure S5 and Table S2.

Next, we delineated M1 and M2 macrophages using CD16/32 and CD206 as markers, respectively (Figure 3B). Flow cytometry demonstrated that MSU alone and MSU plus DRG CM-induced M1 macrophage polarization and sFRP2 KD DRG CM inhibited this increased M1 polarization. M2 macrophages, characterized by CD206-positive staining, were stimulated by MSU treatment but were not significantly different among the CM groups and the vehicle group. Consistently, immunofluorescence images showed increased expression of CD16/32 in the vehicle- and DRG CM-treated BMMs, which was inhibited by sFRP2 KD DRG CM treatment, while no obvious change was observed in the expression of CD206 (Figure 3C) among the different groups. Thus, sFRP2 KD was concluded to inhibit the activation of M1 macrophages stimulated by MSU. Although there was no obvious change in CD206-positive macrophages, sFRP2 KD prevented the downregulation of M2-associated cytokines.

As shown in Figure 3D, MSU treatment did not affect the migration of BMMs, whereas DRG CM significantly induced BMM migration. However, migration was inhibited by sFRP2 KD DRG CM, indicating that sFRP2 is one of the potential chemical components mediating macrophage migration.

Neural modulation of macrophages induces endothelial cell apoptosis

During GA, endothelial cells are activated and impaired by inflammatory mediators. This process is characterized by the release of IL-8 and von Willebrand factor from Weibel-Palade bodies in resting endothelial cells within minutes, followed by a sustained program of gene expression of adhesion molecules and chemokines including E-selectin, intercellular adhesion molecule-1 (ICAM-1), and vascular cell adhesion molecule-1 (VCAM-1) [7, 8].

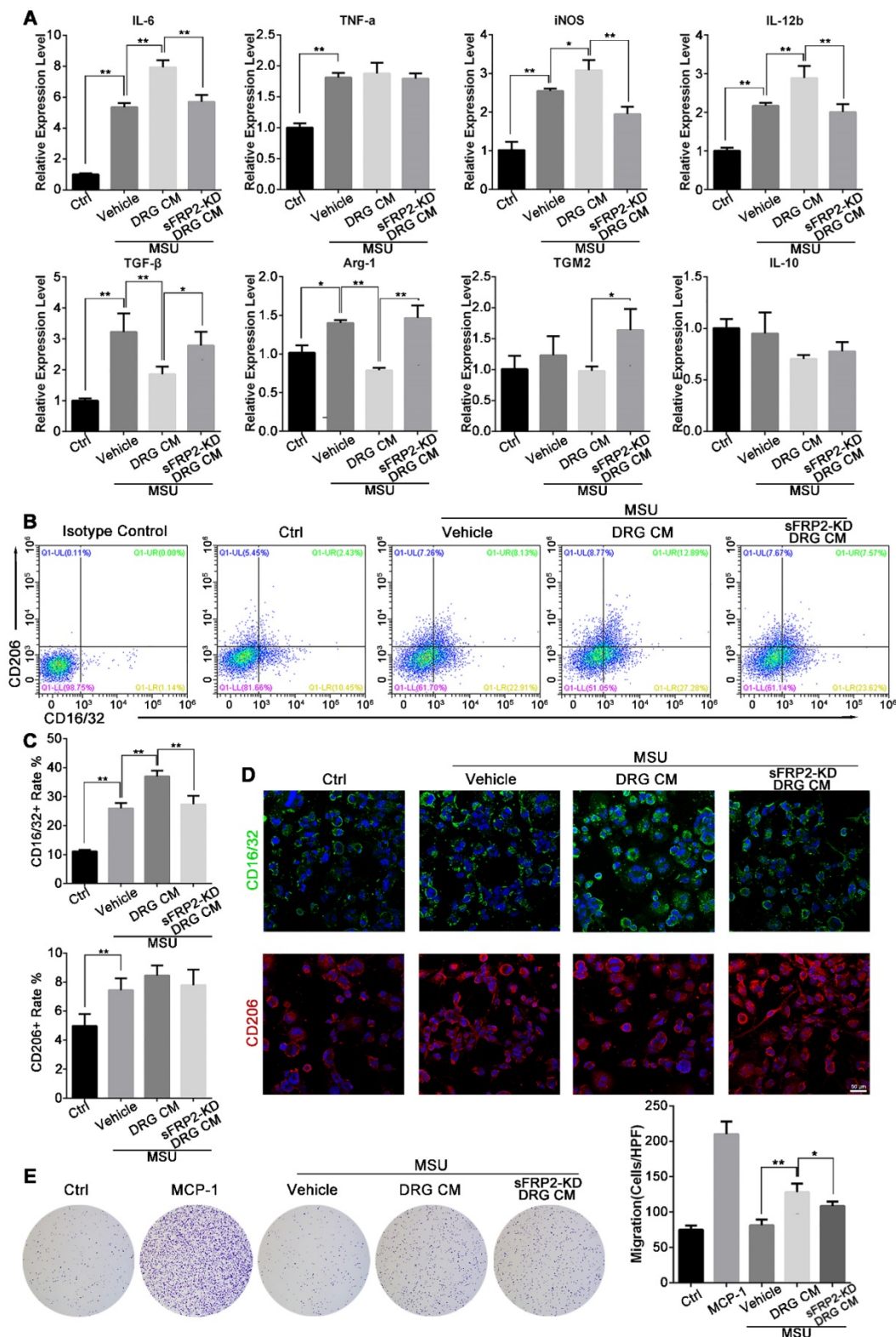


Figure 3. Neural regulation of macrophage polarization and migration. (A), Inflammatory profile of macrophages cultured with MSU alone or MSU plus DRG CM or transduced DRG CM determined by qRT-PCR. (B), Phenotypic characterization of macrophages cultured with MSU alone or MSU plus DRG or transduced DRG CM determined by flow cytometry. Population frequencies of M1 and M2 cells were assessed with CD16/32 and CD206, respectively. (C), Quantitation of CD16/32 and CD206-positive rates of macrophages in response to treatment with MSU alone or MSU plus DRG or transduced DRG CM. (D), Representative images of immunofluorescence staining of macrophages cultured with MSU alone or MSU plus DRG or transduced DRG CM. CD16/32 was used as an M1 marker (green). CD206 was used as an M2 marker (red). Cell nuclei were stained with DAPI (blue). Scale bar, 50 μ m. (E), Representative images depicting crystal violet-stained macrophages that migrated across the membrane of transwell inserts (pore size, 8 μ m) to the lower side after incubation with MSU alone, MSU plus DRG or transduced DRG CM, or 10 ng/mL MCP-1 as a positive control. In vitro experiments were conducted in biological triplicate. Values are the means \pm SD (* P < 0.05 compared with control. ** P < 0.01 compared with control. All statistical significance was determined using one-way ANOVA and Tukey's post comparison test.

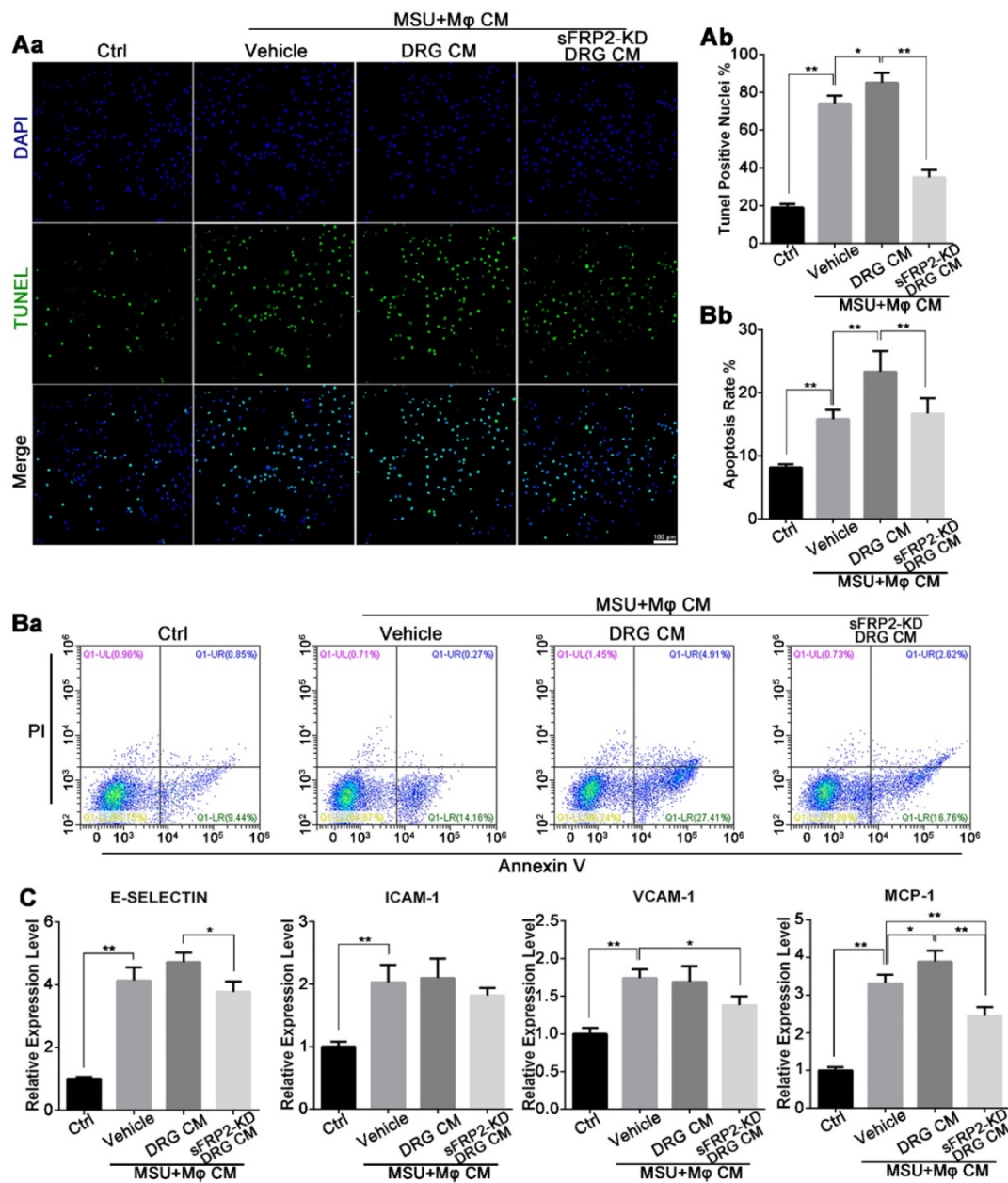


Figure 4. Neural modulation of macrophages induces HUVEC apoptosis. (A), HUVECs cultured with cocultured CM from macrophages and DRG/transduced DRG neurons in the presence of MSU. Apoptosis was assessed by the TUNEL assay in HUVECs. Scale bar, 100 μ m. a. The percentage of TUNEL-positive nuclei was quantified. (B), HUVECs were stained with FITC Annexin V and propidium iodide (PI) for flow cytometry analysis after being cultured with cocultured CM from macrophages and DRG/transduced DRG neurons in the presence of MSU. b. The apoptosis rate was quantified. (C), qRT-PCR was performed to assess the expression of E-selectin, ICAM-1, VCAM-1, and MCP-1 in HUVECs after being cultured with cocultured CM from macrophages and DRG/transduced DRG neurons in the presence of MSU. In vitro experiments were conducted in biological triplicate. Values are the means \pm SD (* P < 0.05 compared with control. ** P < 0.01 compared with control. All statistical significance was determined using one-way ANOVA and Tukey's post comparison test.

To elucidate the changes in endothelial cells, we cultured human umbilical vein endothelial cells (HUVECs) in vitro using coculture media from macrophages together with primary DRG neurons in the presence of MSU crystals. In Figure 4Aa, an increase in the concentration of DNA fragmentation was quantified using a fluorescence TUNEL assay. Compared with the vehicle group, the DRG-macrophage group further exhibited HUVEC apoptosis, whereas the apoptotic rate was inhibited in the sFRP2 KD DRG-macrophage group (Figure 4Ab).

Flow cytometry indicated that the early apoptosis rate was $15.8 \pm 1.5\%$ in the vehicle group, which was higher than the $8.2 \pm 0.4\%$ in the control group. The apoptosis rates of HUVECs were $23.3 \pm 3.3\%$ and $16.7\% \pm 2.4\%$ in the DRG-macrophage group and the sFRP2 KD DRG-macrophage group, respectively (Figure 4Ba and b). This finding indicated that neuroimmune interactions might mediate the apoptosis of HUVECs.

Next, we investigated the gene transcription levels of adhesion molecules and chemokines, including E-selectin, ICAM-1, VCAM-1, and

monocyte chemoattractant protein-1 (MCP-1), which mediate endothelial activation and leukocyte trafficking during gouty attack. The vehicle group (cultured with CM from macrophages in the presence of MSU crystals) expressed significantly higher levels of E-selectin, ICAM-1, VCAM-1, and MCP-1 mRNA than the control group, and the MCP-1 expression level was further increased by CM generated from DRG neurons. Additionally, the sFRP2 KD DRG group expressed lower mRNA levels of adhesion molecules and chemokines than the vehicle group (Figure 4C). Altogether, the above results illustrated that sensory neurons exerted a proinflammatory effect on macrophages mediated by sFRP2 when confronting MSU crystals, consequently leading to more severe endothelial damage and apoptosis.

DRG CM-derived sFRP2 activates the NF- κ B signaling pathway to regulate macrophage polarization

sFRP2, a Wnt-binding protein that is structurally related to Frizzled (Fz), has been shown to regulate Wnt/ β -catenin signal activity. Therefore, we investigated Wnt signaling in macrophages and BMMs in response to MSU crystals to elucidate the process of DRG CM-induced macrophage polarization. First, we screened the mRNA expression levels of Wnt proteins and receptors in BMMs. Wnt7b, Wnt9a, Wnt9b, frizzled 2 (FZD2), and low-density lipoprotein receptor-related protein 5 (LRP5) were the most promoted genes after MSU stimulation (Figure S6). Figure 5A shows that Wnt/ β -catenin activation was significantly induced by CM from sFRP2 KD DRG neurons. Compared to the control treatment, MSU stimulated the expression of Wnt9a, FZD2, dishevelled-2 (DVL2), and β -catenin, along with the downstream c-myc and cyclin D1, which were further activated after treatment with sFRP2 KD DRG CM combined with MSU (except for DVL2 and cyclin D1). These results implied that MSU significantly upregulated the expression of Wnt9a and receptor FZD2, potentially sensitizing the Wnt signal in macrophages. Thus, β -catenin expression was evaluated in the MSU group. The absence of DRG-derived sFRP2 further removed the inhibitory effect on Wnt signaling in macrophages. The expression of β -catenin was further upregulated in the sFRP2 KD DRG CM group compared with that in the DRG CM group. Therefore, we hypothesized that the DRG modulation effect on macrophages was probably due to the regulation of Wnt signaling via sFRP2. In Figure 5B, upregulation of FZD2 in BMMs after treatment with MSU and sFRP2 KD DRG CM

was found, implying a crucial role for Wnt/FZD signaling in macrophages in response to neural modulation. These results suggested that sFRP2 inhibited Wnt activity in macrophages that was activated by MSU stimulation during GA.

NF- κ B has been shown to be a significant transcription factor that regulates macrophage polarization in response to inflammatory cytokines, infection and stress [35]. To examine the possibility that Wnt modulated the activation of NF- κ B, the selective Wnt/ β -catenin signaling inhibitor ICG-001 was used. The process of NF- κ B activation requires phosphorylation of I κ B α by I κ B kinase (IKK) followed by degradation in a proteasome, which leads to subsequent p65 nuclear translocation. Figure 5C shows that MSU (group 2) and DRG CM (group 3) upregulated the expression of p-I κ B α compared with control treatment (group 1), and this upregulation was inhibited in the sFRP2 KD DRG CM group (group 4). However, extra administration of ICG-001 (group 5) rescued the p-I κ B α level. These results implied that sFRP2, as an antagonist that prevents Wnt/ β -catenin signal activation, activates the NF- κ B signaling pathway. Specifically, Figure 5D and 5E illustrate that MSU induced the nuclear translocation of p65 and that DRG CM further promoted this nuclear translocation, potentially due to the inactivation of NF- κ B via sFRP2. Additionally, when cultured in sFRP2 KD DRG CM, the translocation level of p65 was significantly inhibited, and this inhibition was rescued by ICG-001. More importantly, pulldown assay results demonstrated that β -catenin formed a complex with p65 in the MSU plus DRG CM group, which possibly attenuated p65 translocation (Figure 5F).

These data indicated that DRG-derived sFRP2 inhibited Wnt/ β -catenin signaling with decreased stabilization of β -catenin in macrophages, further promoting the nuclear translocation of the NF- κ B p65 subunit and subsequent transcriptional activity.

Discussion

Neurogenic inflammation exhibited as orchestrated actions of inflammatory cells, vascular cells, and neurons provoked by pathological conditions and increased neuronal activity [36], blur the boundaries between the immune and nervous system. For instance, recent studies have demonstrated that TLRs 3, 4, 7, and 9 in the human/mouse DRG mediate the production of proinflammatory chemokines and sensitization of nociceptors [37-39].

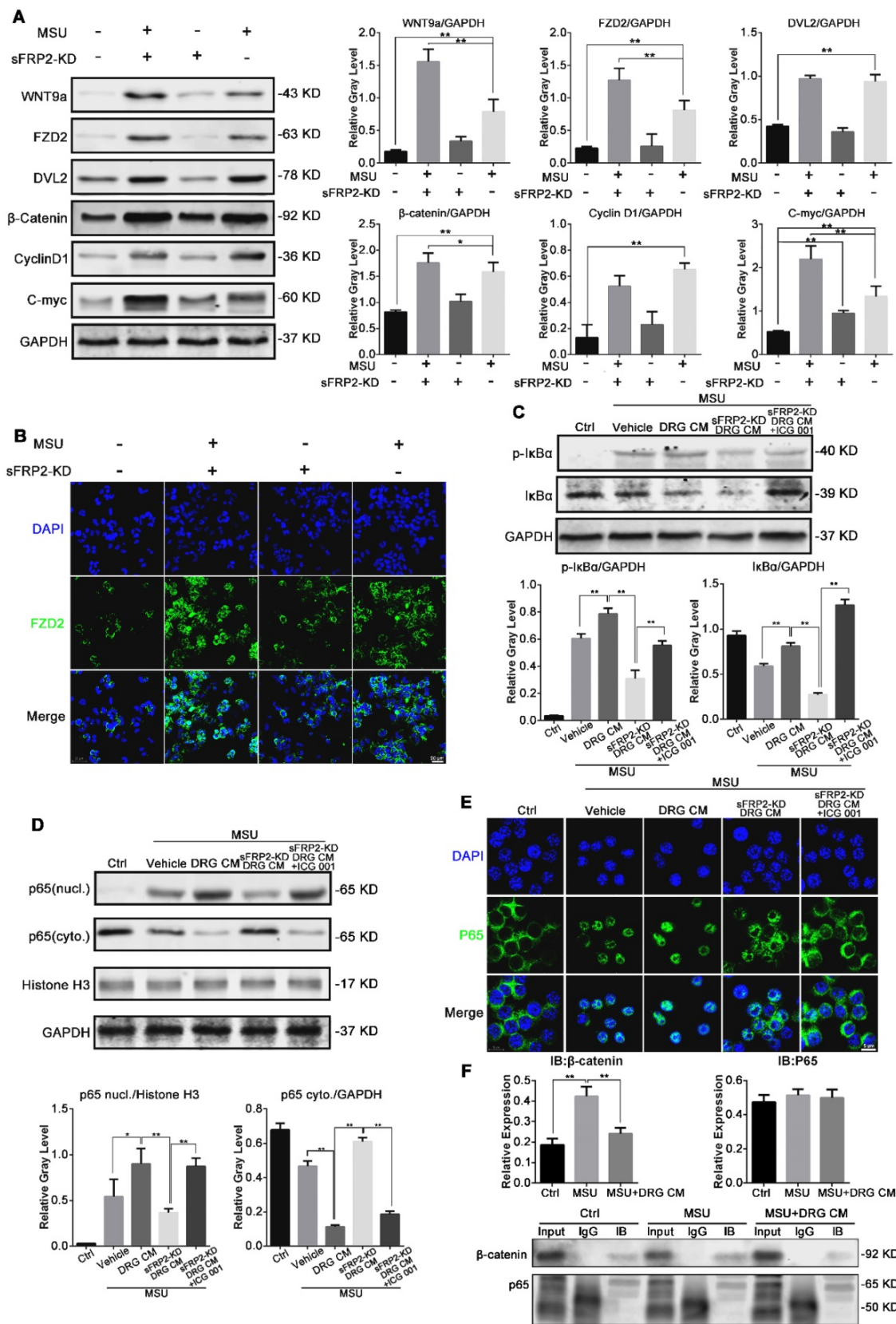


Figure 5. The Wnt/β-catenin signaling pathway controls BMM inflammation in response to MSU crystals. (A), Western blot analysis of lysates from macrophages cultured with MSU and DRG/transduced DRG CM and probed with antibodies as indicated. (B), Representative images of immunofluorescence staining of macrophages cultured with DRG/transduced DRG CM. The panels on the 2nd line show FZD2 expression levels (green). Cell nuclei were stained with DAPI (blue). Scale bar, 20 μm. (C), Western blot analysis of lysates from macrophages cultured with MSU and DRG CM, transduced DRG CM, or transduced DRG CM plus 3 μM ICG-001 and probed with antibodies as indicated. (D), Macrophages were pretreated with MSU and DRG CM, transduced DRG CM, or transduced DRG CM plus 3 μM ICG-001. (E), Nuclear translocation of p65 was visualized using immunofluorescence. Scale bar, 10 μm. (F), Co-immunoprecipitation of β-catenin with p65 in macrophages.

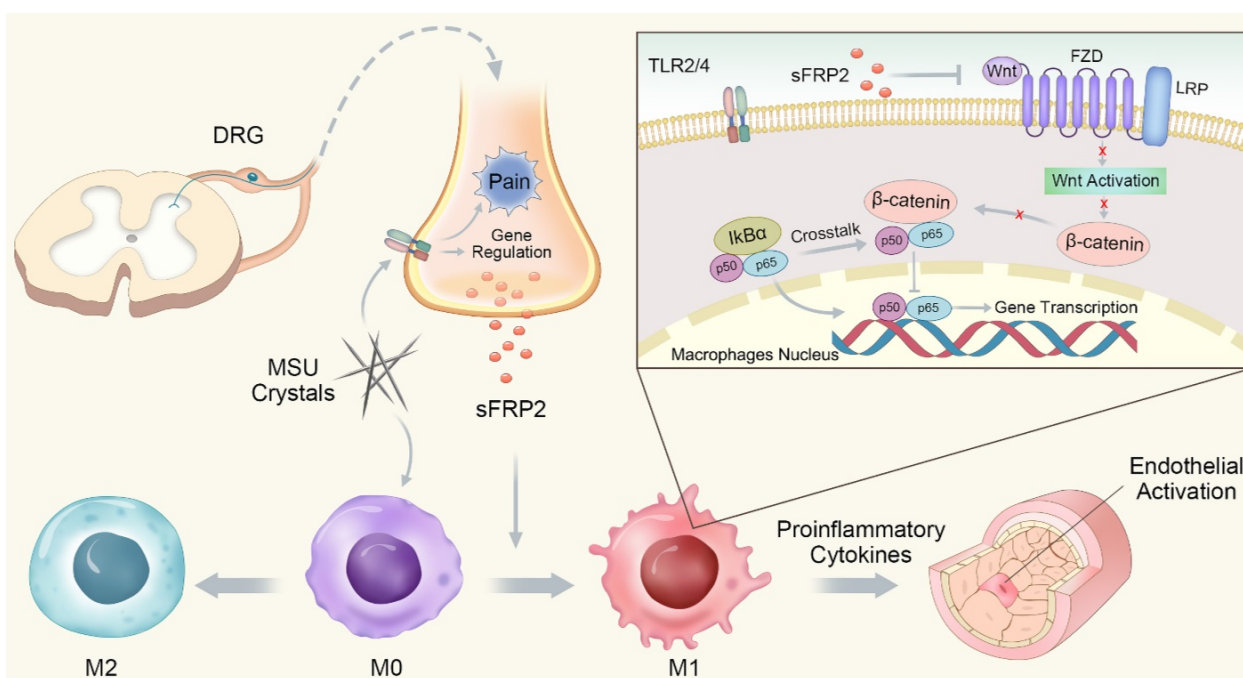


Figure 6. Schematic illustration of the role of DRG neuron-derived sFrp2 in GA.

More shared receptors, such as transient receptor potential (TRP) ion channels and purinergic receptors, could be activated by major cytokines released from immune cells [40, 41], causing a secondary release of neuropeptides at peripheral terminals that further activate inflammatory cells [15], resulting in positive feedback that facilitates inflammation. The specific combination of signaling chemokines tightly coordinates the nervous and immune system, exerting either anti-inflammatory or deleterious inflammatory aspects in response to infection or noxious stimuli [42]. Studies have shown that TNF- α has an influential and extensive but poorly understood effect on the autoimmune response in rheumatoid arthritis (RA) [43]. Recently, Koopman et al. extended the data to the clinic, showing that vagus nerve stimulation attenuated disease severity by inhibiting TNF- α [44].

Here, we demonstrated a novel sensory nerve-macrophage-vascular endothelium axis mediated by DRG sFrp2 that regulates the inflammatory process of GA. Specifically, lentiviral vectors were delivered to DRG cell soma innervating MSU-deposited tissue, resulting in the inhibition of sFrp2 in both soma and fibers. SFRP2 was hypothesized to be a candidate in mediating the interaction between sensory neurons and macrophages. SFRP2 KD in the DRG inhibited inflammatory cell infiltration and M1 macrophage polarization in the synovial membrane of MSU-induced GA mice. During GA, DRG neurons facilitated the in situ inflammation response by secreting sFrp2.

SFRPs are a family of soluble Wnt antagonists that are postulated to be homogenous with the proposed Wnt-binding region on Fz proteins [45]. Extensive studies have led to the concept that Wnt/ β -catenin signaling reciprocally regulates inflammation to reconstitute tissue homeostasis [46]. For instance, P. Zhang showed that Wnt/ β -catenin activation in macrophages inhibited inflammation against tularemia [47]. Additionally, alarmins S100A8/A9 induced canonical Wnt signaling in macrophages, resulting in decreased expression of matrix metalloproteinase 3 (MMP-3) and IL-6. In GA, Wnt5a and its receptor FZD5 in macrophages are mediated by NF- κ B and TLR2/4 [48], which are involved in MSU recognition to trigger the downstream NACHT, LRR, and PYD domains-containing protein (NALP3) inflammasome in human macrophages [10]. Herein, we showed that MSU significantly promoted Wnt9a, FZD2 and β -catenin expression in murine macrophages. Interestingly, sFrp2 in DRG CM exhibited a robust stimulating effect of p65 nuclear translocation in macrophages, indicating that the absence of Wnt activation resulted in a more severe inflammatory response.

The action of sFrp2 on Wnt/ β -catenin has been demonstrated to differ depending on the tissue system. Human studies have shown that increased expression of sFrp2 activates β -catenin signaling in melanocytes, resulting in increased melanogenesis [49]. However, in esophageal adenocarcinoma and Barrett's esophagus, aberrant promoter methylation

might functionally silence sFRP2 gene expression, which has been implicated in activation of the Wnt signaling pathway and acquisition of aggressive tumor behavior [50]. In this study, inhibition of sFRP2 mimicked the induction of Wnt signaling in macrophages, resulting in accumulation of β -catenin and upregulation of its downstream genes, including cyclin D1 and c-myc, which have been reported to govern macrophage adhesion and motility [51].

The NF- κ B pathway has emerged as a regulator of the elicitation of the macrophage polarization response. NF- κ B (a homo/heterodimer consisting of the p65 and p50 protein) is restricted in its inactive form by I κ B and targets gene transcription in response to proinflammatory cytokines or microbial-associated molecular patterns. Many M1 genes have NF- κ B sites in their promoter region, including IL-6, iNOS, and MCP-1. Additionally, p50 NF- κ B homodimers were found to orchestrate the M2 phenotype and repress the expression of M1 cytokines [52, 53]. We discovered that DRG-derived sFRP2 activated NF- κ B in macrophages, resulting in an increase in proinflammatory gene expression and reduction in M2-associated cytokine expression. The data indicated that DRG-derived sFRP2 inhibited MSU-activated Wnt/ β -catenin signaling with decreased stabilization of β -catenin in macrophages. Therefore, less stabilized β -catenin was involved in the interaction with the NF- κ B p65 subunit, promoting the nuclear translocation of the NF- κ B p65 subunit and the following transcriptional activity, making sFRP2 a suitable therapeutic target for the treatment of GA. Deng J. first reported evidence that β -catenin can physically complex with p65, resulting in a reduction in NF- κ B DNA binding and oncogenesis of human colon and breast cancer [54]. In intestinal stem cells, β -catenin was induced by the Salmonella effector protein AvrA during an infection and then interacted with the NF- κ B p50 subunit, decreasing its transcriptional activity [55]. However, an in vitro pulldown assay showed that β -catenin did not interact with either p65 or p50 alone, indicating that β -catenin was able to complex with p65 only with cellular factors [56].

As a mean of alleviating pain and minimizing the side effects, the regional therapeutic approach, particularly targeting DRG, represent a safer alternative to systemic administration of therapeutic agents [57]. Compared to the serious challenge of the blood-brain barrier in CNS, the higher permeability and perfusion rates in DRG allow the easy diffusion of large molecular weight compounds and the accessibility of nanoparticles designed for diagnostics and therapeutics.

In conclusion, we determined that sFRP2, as a factor released from DRG neurons, contributes to inflammation by promoting macrophage M1 polarization and migration via the regulation of the Wnt/ β -catenin and NF- κ B signaling pathways. The proinflammatory cytokines subsequently induce endothelial activation and apoptosis (Figure 6). This study capitalized on a new understanding of peripheral sensory nerve function in GA and proposed the increased sFRP2 in DRG was a potential target for the prevention and treatment of GA.

Abbreviations

sFRP2, secreted frizzled related protein 2; GA, gouty arthritis; DRG, dorsal root ganglion; MSU, monosodium urate; CNS, central nervous system; BMM, bone marrow-derived macrophages; KD, knockdown; CM, conditioned medium.

Supplementary Material

Supplementary figures and tables.

<http://www.thno.org/v09p3707s1.pdf>

Acknowledgments

This work was supported by the National Natural Science Foundation of China (81672205), National Key R&D Programme (2016YFC1102100) and the Shanghai Science and Technology Development Fund (18DZ2291200, 18441902700).

Author contributions

J.M. and F.Z. contributed equally to this work. J.M., F.Z., H.Q., HanJun L. designed the experiment. J.M. and F.Z. collected and analyzed the data. J.M., H.Q., T.T. contributed to the interpretation of the results and critical revision of the manuscript for important intellectual content and approved the final version of the manuscript. All authors meet the International Committee of Medical Journal Editors recommendations. All authors have critically reviewed the manuscript.

Data and materials availability

All data needed to evaluate the conclusions in the paper are present in the paper and/or the Supplementary Materials. Additional data related to this paper may be requested from the authors.

Competing Interests

The authors have declared that no competing interest exists.

References

1. Kuo C-F, Grainge MJ, Zhang W, Doherty M. Global epidemiology of gout: prevalence, incidence and risk factors. *Nat Rev Rheumatol*. 2015; 11: 649.

2. Dalbeth N, Merriman TR, Stamp LK. Gout. *The Lancet*. 2016; 388: 2039-52.
3. Zhou Q, Lin FF, Liu SM, Sui XF. Influence of the total saponin fraction from *Dioscorea nipponica* Makino on TLR2/4-IL1R receptor signal pathway in rats of gouty arthritis. *J Ethnopharmacol*. 2017; 206: 274-82.
4. Gallo J, Raska M, Kriegova E, Goodman SB. Inflammation and its resolution and the musculoskeletal system. *J Orthop Translat*. 2017; 10: 52-67.
5. Wang N, Liang H, Zen K. Molecular mechanisms that influence the macrophage m1-m2 polarization balance. *Front Immunol*. 2014; 5: 614.
6. Liao WT, You HL, Li C, Chang JG, Chang SJ, Chen CJ. Cyclic GMP-dependent protein kinase II is necessary for macrophage M1 polarization and phagocytosis via toll-like receptor 2. *J Mol Med (Berl)*. 2015; 93: 523-33.
7. Wolff B, Burns AR, Middleton J, Rot A. Endothelial cell "memory" of inflammatory stimulation: human venular endothelial cells store interleukin 8 in Weibel-Palade bodies. *J Exp Med*. 1998; 188: 1757-62.
8. Haskard DO, Landis RC. Interactions between leukocytes and endothelial cells in gout: lessons from a self-limiting inflammatory response. *Arthritis Res*. 2002; 4 Suppl 3: S91-S7.
9. Martinez FO, Helming L, Gordon S. Alternative Activation of Macrophages: An Immunologic Functional Perspective. *Annu Rev Immunol*. 2009; 27: 451-83.
10. Cronstein BN, Terkeltaub R. The inflammatory process of gout and its treatment. *Arthritis Res Ther*. 2006; 8 Suppl 1: S3-S.
11. Chen YH, Hsieh SC, Chen WY, Li KJ, Wu CH, Wu PC, et al. Spontaneous resolution of acute gouty arthritis is associated with rapid induction of the anti-inflammatory factors TGFbeta1, IL-10 and soluble TNF receptors and the intracellular cytokine negative regulators CIS and SOCS3. *Ann Rheum Dis*. 2011; 70: 1655-63.
12. Ortiz-Bravo E, Sieck MS, Schumacher HR, Jr. Changes in the proteins coating monosodium urate crystals during active and subsiding inflammation. Immunogold studies of synovial fluid from patients with gout and of fluid obtained using the rat subcutaneous air pouch model. *Arthritis Rheum*. 1993; 36: 1274-85.
13. Ariel A, Fredman G, Sun YP, Kantarci A, Van Dyke TE, Luster AD, et al. Apoptotic neutrophils and T cells sequester chemokines during immune response resolution through modulation of CCR5 expression. *Nat Immunol*. 2006; 7: 1209-16.
14. Akahoshi T, Nagaoka T, Namai R, Sekiyama N, Kondo H. Prevention of neutrophil apoptosis by monosodium urate crystals. *Rheumatol Int*. 1997; 16: 231-5.
15. Chiu IM, von Hehn CA, Woolf CJ. Neurogenic inflammation and the peripheral nervous system in host defense and immunopathology. *Nat Neurosci*. 2012; 15: 1063.
16. Chavan SS, Tracey KJ. Essential Neuroscience in Immunology. *J Immunol*. 2017; 198: 3389.
17. Ren K, Dubner R. Interactions between the immune and nervous systems in pain. *Nat Med*. 2010; 16: 1267-76.
18. Segond von Banchet G, Boettger MK, Fischer N, Gajda M, Bräuer R, Schaible H-G. Experimental arthritis causes tumor necrosis factor- α -dependent infiltration of macrophages into rat dorsal root ganglia which correlates with pain-related behavior. *Pain*. 2009; 145: 151-9.
19. Chiu IM, Heesters BA, Ghasemlou N, Von Hehn CA, Zhao F, Tran J, et al. Bacteria activate sensory neurons that modulate pain and inflammation. *Nature*. 2013; 501: 52.
20. Borovikova LV, Ivanova S, Zhang M, Yang H, Botchkina GI, Watkins LR, et al. Vagus nerve stimulation attenuates the systemic inflammatory response to endotoxin. *Nature*. 2000; 405: 458.
21. Trevisan G, Hoffmeister C, Rossato MF, Oliveira SM, Silva MA, Ineu RP, et al. Transient receptor potential ankyrin 1 receptor stimulation by hydrogen peroxide is critical to trigger pain during monosodium urate-induced inflammation in rodents. *Arthritis Rheum*. 2013; 65: 2984-95.
22. Berta T, Qadri Y, Tan PH, Ji RR. Targeting dorsal root ganglia and primary sensory neurons for the treatment of chronic pain. *Expert Opin Ther Targets*. 2017; 21: 695-703.
23. Abram SE, Yi J, Fuchs A, Hogan QH. Permeability of injured and intact peripheral nerves and dorsal root ganglia. *Anesthesiology*. 2006; 105: 146-53.
24. Jorge LL, Feres CC, Teles VE. Topical preparations for pain relief: efficacy and patient adherence. *J Pain Res*. 2010; 4: 11-24.
25. Chen G, Park CK, Xie RG, Ji RR. Intrathecal bone marrow stromal cells inhibit neuropathic pain via TGF-beta secretion. *J Clin Invest*. 2015; 125: 3226-40.
26. Dorn G, Patel S, Wotherspoon G, Hemmings-Mieszczyk M, Barclay J, Natt FJ, et al. siRNA relieves chronic neuropathic pain. *Nucleic Acids Res*. 2004; 32: e49.
27. MacDonald BT, Tamai K, He X. Wnt/beta-catenin signaling: components, mechanisms, and diseases. *Dev Cell*. 2009; 17: 9-26.
28. Kawano Y, Kypta R. Secreted antagonists of the Wnt signalling pathway. *J Cell Sci*. 2003; 116: 2627-34.
29. Martin WJ, Walton M, Harper J. Resident macrophages initiating and driving inflammation in a monosodium urate monohydrate crystal-induced murine peritoneal model of acute gout. *Arthritis Rheum*. 2009; 60: 281-9.
30. Glatzel M, Flechsig E, Navarro B, Klein MA, Paterna JC, Bueler H, et al. Adenoviral and adeno-associated viral transfer of genes to the peripheral nervous system. *Proc Natl Acad Sci U S A*. 2000; 97: 442-7.
31. Chaplan SR, Bach FW, Pogrel JW, Chung JM, Yaksh TL. Quantitative assessment of tactile allodynia in the rat paw. *J Neurosci Methods*. 1994; 53: 55-63.
32. Han Q, Bing W, Di Y, Hua L, Shi-He L, Yu-Hua Z, et al. Kinsenoside screening with a microfluidic chip attenuates gouty arthritis through inactivating NF- κ B signaling in macrophages and protecting endothelial cells. *Cell Death Dis*. 2016; 7: e2350.
33. Li H, Liu P, Xu S, Li Y, Dekker JD, Li B, et al. FOXP1 controls mesenchymal stem cell commitment and senescence during skeletal aging. *J Clin Invest*. 2017; 127: 1241-53.
34. Day IN, Hinks LJ, Thompson RJ. The structure of the human gene encoding protein gene product 9.5 (PGP9.5), a neuron-specific ubiquitin C-terminal hydrolase. *Biochem J*. 1990; 268: 521.
35. Mancino A, Lawrence T. Nuclear factor-kappaB and tumor-associated macrophages. *Clin Cancer Res*. 2010; 16: 784-9.
36. Xanthos DN, Sandkuhler J. Neurogenic neuroinflammation: inflammatory CNS reactions in response to neuronal activity. *Nat Rev Neurosci*. 2014; 15: 43-53.
37. Qi J, Buzas K, Fan H, Cohen JJ, Wang K, Mont E, et al. Painful Pathways Induced by TLR Stimulation of Dorsal Root Ganglion Neurons. *J Immunol*. 2011; 186: 6417-26.
38. Jung WJ, Lee SY, Choi SI, Kim BK, Lee EJ, In KH, et al. Toll-like receptor expression in pulmonary sensory neurons in the bleomycin-induced fibrosis model. *PLoS ONE*. 2018; 13: e0193117.
39. Chen T, Li H, Yin Y, Zhang Y, Liu Z, Liu H. Interactions of Notch1 and TLR4 signaling pathways in DRG neurons of in vivo and in vitro models of diabetic neuropathy. *Sci Rep*. 2017; 7: 14923.
40. Parenti A, De Logu F, Geppetti P, Benemei S. What is the evidence for the role of TRP channels in inflammatory and immune cells? *Br J Pharmacol*. 2016; 173: 953-69.
41. Dubyak GR, el-Moatassim C. Signal transduction via P2-purinergic receptors for extracellular ATP and other nucleotides. *Am J Physiol Cell Physiol*. 1993; 265: C577-C606.
42. Chavan SS, Pavlov VA, Tracey KJ. Mechanisms and Therapeutic Relevance of Neuro-immune Communication. *Immunity*. 2017; 46: 927-42.
43. Matsuno H, Yudoh K, Katayama R, Nakazawa F, Uzuki M, Sawai T, et al. The role of TNF-alpha in the pathogenesis of inflammation and joint destruction in rheumatoid arthritis (RA): a study using a human RA/SCID mouse chimera. *Rheumatology (Oxf)*. 2002; 41: 329-37.
44. Koopman FA, Chavan SS, Miljko S, Grazio S, Sokolovic S, Schuurman PR, et al. Vagus nerve stimulation inhibits cytokine production and attenuates disease severity in rheumatoid arthritis. *Proc Natl Acad Sci U S A*. 2016; 113: 8284-9.
45. Bovolenta P, Esteve P, Ruiz JM, Cisneros E, Lopez-Rios J. Beyond Wnt inhibition: new functions of secreted Frizzled-related proteins in development and disease. *J Cell Sci*. 2008; 121: 737-46.
46. Schaale K, Neumann J, Schneider D, Ehlers S, Reiling N. Wnt signaling in macrophages: augmenting and inhibiting mycobacteria-induced inflammatory responses. *Eur J Cell Biol*. 2011; 90: 553-9.
47. Zhang P, Katz J, Michalek SM. Glycogen synthase kinase-3beta (GSK3beta) inhibition suppresses the inflammatory response to Francisella infection and protects against tularemia in mice. *Mol Immunol*. 2009; 46: 677-87.
48. Blumenthal A, Ehlers S, Lauber J, Buer J, Lange C, Goldmann T, et al. The Wingless homolog WNT5A and its receptor Frizzled-5 regulate inflammatory responses of human mononuclear cells induced by microbial stimulation. *Blood*. 2006; 108: 965.
49. Kim M, Han JH, Kim JH, Park TJ, Kang HY. Secreted Frizzled-Related Protein 2 (sFRP2) Functions as a Melanogenic Stimulator; the Role of sFRP2 in UV-Induced Hyperpigmentary Disorders. *J Invest Dermatol*. 2016; 136: 236-44.
50. Saito T, Mitomi H, Imamhasan A, Hayashi T, Mitani K, Takahashi M, et al. Downregulation of sFRP-2 by epigenetic silencing activates the beta-catenin/Wnt signaling pathway in esophageal basaloid squamous cell carcinoma. *Virchows Arch*. 2014; 464: 135-43.

51. Neumeister P, Pixley FJ, Xiong Y, Xie H, Wu K, Ashton A, et al. Cyclin D1 Governs Adhesion and Motility of Macrophages. *Mol Biol Cell*. 2003; 14: 2005-15.
52. Brasier AR. The nuclear factor-kappaB-interleukin-6 signalling pathway mediating vascular inflammation. *Cardiovasc Res*. 2010; 86: 211-8.
53. Huang W, Ghisletti S, Perissi V, Rosenfeld MG, Glass CK. Transcriptional integration of TLR2 and TLR4 signaling at the NCoR derepression checkpoint. *Mol Cell*. 2009; 35: 48-57.
54. Deng J, Miller SA, Wang HY, Xia W, Wen Y, Zhou BP, et al. beta-catenin interacts with and inhibits NF-kappa B in human colon and breast cancer. *Cancer Cell*. 2002; 2: 323-34.
55. Liu X, Lu R, Wu S, Sun J. Salmonella regulation of intestinal stem cells through the Wnt/beta-catenin pathway. *FEBS Lett*. 2010; 584: 911-6.
56. Deng J, Miller SA, Wang H-Y, Xia W, Wen Y, Zhou BP, et al. β -catenin interacts with and inhibits NF- κ B in human colon and breast cancer. *Cancer Cell*. 2002; 2: 323-34.
57. Sapunar D, Kostic S, Banozic A, Puljak L. Dorsal root ganglion - a potential new therapeutic target for neuropathic pain. *J Pain Res*. 2012; 5: 31-8.